Numerical Study of Thermally Targeted Liposomal Drug Delivery in Tumor

Aili Zhang
Xipeng Mi
Geer Yang

Department of Biomedical Engineering,
Shanghai Jiao Tong University,
Shanghai 200240, P.R. China

Lisa X. Xu
Department of Biomedical Engineering,
and Med-X Research Institute,
Shanghai Jiao Tong University,
Shanghai 200240, P.R. China

The efficacy of cancer chemotherapy can be greatly enhanced by thermally targeted nanoparticle liposome drug delivery system. A new theoretical model coupling heat and mass transfer has been developed to study the spatial and transient drug distributions. In this model, the influence of tumor cell apoptosis and necrosis in drug transport is also considered, in addition to the tumor microvasculature permeability to nanoliposomes. The model predictions agree well with our previous experimental results, and it has been used to simulate the nanoparticle drug distribution in the tumor under hyperthermic conditions. Results show that hyperthermia alone only enhances drug accumulation in the periphery of a tumor with 1 cm in radius, and the tumor cells in the central region are hardly damaged due to poor drug diffusion. Apoptosis or necrosis of the tumor cells could significantly influence the drug penetration and should be accounted for in drug diffusion modeling to accurately predict the therapeutic effect. Simulation study on the combined radio frequency ablation and liposomal doxorubicin delivery shows more effective treatment outcome, especially for larger tumors. The present model can be used to predict the treatment outcome and optimize the clinical protocol.
[DOI: 10.1115/1.3072952]

Keywords: thermally targeted drug delivery, hyperthermia, nanoparticle liposomes, RF ablation

1 Introduction

Improvement of the therapeutic efficacy while minimizing the side effects of antitumor drug on normal healthy tissues has been a long struggling goal of many researchers. Encapsulating drug with liposomes of certain sizes is proven to prolong the drug circulation time, reduce the drug accumulation in normal tissues, and thus, enhance the targeted drug delivery to the tumor [1,2]. This is in part attributed to the incomplete and leaky wall of the vessels in a tumor. The optimal liposome size is found to be between 90 nm and 200 nm in diameter, as both the circulation time and accumulation in the tumor are considered [3,4].

To further increase the antitumor drug delivery efficiency, mild heating (i.e., hyperthermia) is used locally. Study of the thermally targeted liposomal drug delivery has been reported to enhance antitumor efficacy [5,6]. During hyperthermia, the local blood perfusion and the permeability of the tumor vasculature to macromolecules are significantly increased, resulting in massive extravasation of nanoparticle liposomal drug [7–10]. Moreover, thermally sensitive liposomes can also be used to release drug at the locally elevated temperature for better therapeutic index [11,12]. The final outcome of the chemotherapeutic treatment depends on an adequate drug distribution throughout the tumor. Survival of some tumor cells might lead to tumor recurrence or metastasis. However, it is very difficult to observe the local drug concentration in vivo even with the most advanced imaging techniques. Thus, modeling and numerical simulations of the drug delivery process become necessary and useful.

Several models have been developed to describe the drug delivery process for different applications [13–15]. Ward et al. studied the drug transport and tumor growth at the same time using a mathematical model to describe small molecules drug and nutrition transported from the tumor edge to the center through diffusion only (no advection through vascular network taken into account). Considering the characteristics of breast cancer, Lankelma et al. [16,17] studied the doxorubicin activity in islets of breast cancer by assuming drug transport through both transcellular (the cellular network) and paracellular (the intercellular interstitium) pathways. Magni et al. [18] built a mathematical model to describe the cancer growth dynamics in response to anticancer agents in xenograft. In this model, the tumor cell growth, division, and death are all considered, and the change of tumor in response to chemotherapy is assumed to be determined by the balance between the cell proliferation and death. El-Kareh and Secomb [19–21] presented models accounting for the cellular pharmacodynamics of drug, and numerically studied the intraperitoneal delivery of cisplatin in tumor and investigated the influence of hyperthermia on the drug penetration distance.

Unlike small molecule drug transport, the delivery process of liposomal drug is much more complex. The liposome encapsulated drug selectively extravasates into the tumor region from blood vessels [22]. Hyperthermia has been found to remarkably improve the extravasation of liposome nanoparticles [4,12]. As the liposome breaks, the antitumor drug releases and diffuses throughout the tumor region. Without taking the spatial nonuniformity of the tumor into consideration, El-Kareh and Secomb [23] developed a model to compare the different delivery methods of bolus injection, continuous infusion, and liposomal delivery of doxorubicin. The model has been used to study the liposome leakage from the tumor vasculature, the breakage of liposomes, and the cellular uptake of free drug simultaneously, but the diffusion effect is neglected. In fact, the heterogeneous distribution of tumor vessels causes nonuniform extravasation of liposomal drugs, which could in turn significantly affect the drug concentration gradient [24]. The effect of tumor cell necrosis and apoptosis induced by the antitumor drugs [25] should also be considered in modeling. Furthermore, as local heating is imposed on the tumor,

Contributed by the Heat Transfer Division of ASME for publication in the JOURNAL OF HEAT TRANSFER. Manuscript received September 9, 2008; final manuscript received December 9, 2008; published online February 24, 2009. Review conducted by Robert D. Tzou. Paper presented at the 2008 International Conference on Micro/Nanoscale Heat Transfer (MNHT2008), Tainan, Taiwan, January, 6–9, 2008.

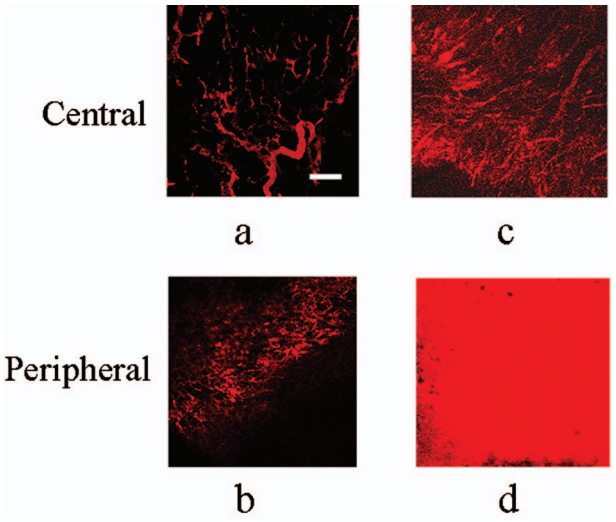

Fig. 1 Vasculature fluorescent images in the tumor center and periphery before and after thermal treatments. Bar: 200 μm. (*a*) and (*b*): before treatment and (*c*) and (*d*): heated at 42°C for 1 h [8].

tissue temperature distributions are normally not uniform, and the drug delivery is coupled with heat and mass transfer.

To precisely study the liposomal delivery and free drug distribution inside the tumor during hyperthermia, the coupled heat and mass transport process has been investigated and modeled based on our previous experimental results. In this model, the heterogeneous tumor morphology, vascular permeability to liposome nanoparticles, and the drug gradients are all considered. The treatment efficacy is quantified and compared with the experimental results. Influences of some key parameters, such as the liposome rupture rate, the apoptosis induced diffusivity change on drug penetration, are studied. The model is further used to investigate the radio frequency (RF) ablation combined liposome drug treatment for larger tumors by coupling heat and mass transfer.

2 Experimental Study of Nanoparticle Liposome Extravasation In Vivo

In our previous experimental study, the extravastion of liposomes in the 4T1 tumor of nude mice has been quantified, and the microvascular sensitivity to hyperthermia studied [8]. Tumor is implanted into the skin tissue within the window chamber on the dorsal flap of the nude mouse. After 10 days of growth, the tumor becomes 1–2 mm in diameter and 150 μm thick. Densely distributed and incomplete angiogenesis is found in the tumor peripheral region, while there are only few vessels in a more ordered branching pattern in the tumor central region through histological study. The vasculature in the tumor peripheral region is found to be much more sensitive to hyperthermia than that in the center. Stabilized long-circulating polyethyleneglycol (PEG) liposome is prepared by the lipid film hydration and extrusion method. Liposome with a narrow size distribution (average of 90–120 nm) has been used. A 200 ul suspension of the liposomal doxorubicin (encapsulated Dox of concentration 0.1 mg/ml) is injected into the tail vein of the anesthetized mouse (average weight of 20 g). The tumor is heated to 42°C using a water bath mounted to the window chamber for 1 h, and the temperatures are monitored using thermocouples. The extravasation of liposomes are observed and imaged by confocal microscopy shown in Fig. 1. The fluorescence intensity indicating the liposome concentration in the tumor interstitial is quantified three-dimensionally and results are compared with those without heating (when the mouse body temperature at 34°C), as shown in Fig. 2.

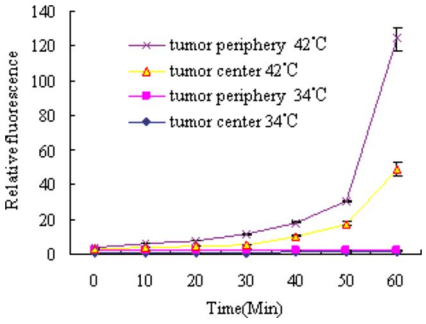

Fig. 2 HT-induced extravasation of 100 nm liposome nanoparticles at 42°C or 34°C for 1 h in different tumor regions. The largest HT enhancement of extravasation was seen at tumor periphery. Values are mean and standard error (SE) (n=11 for each group) [8].

As seen in Fig. 2, hyperthermia has caused a large increase in liposomal Dox extravasation in the peripheral region, while only a small increase is found in the tumor center as compared with those at the body temperature. Different thermal sensitivities of the newly formed and incomplete vessels in the tumor periphery and the relatively mature vascular network could have contributed to the heterogeneous extravasation of the nanoparticle liposomal drug.

3 Model Development

As previously observed in our experimental studies [8], few vessels exist in the central region of the tumor, while abundant vessels are found in the peripheral region. For modeling purposes, a tumor with radius of R can be divided into two parts: the central region within $r<R_c$ without any vessels and the peripheral region of $R_c<r<R$ with microvasculature evenly distributed, as illustrated in Fig. 3. The surrounding normal tissue is assumed to be infinite.

The liposomal doxorubicin is injected through the rat tail vein, and transports in the vasculature before reaching the tumor. Due to the elimination effect, the liposome concentration in plasma decreases exponentially with time and can be expressed as [23]

$$C_{L,V}=\frac{M}{M_g}(A_1e^{-k_1t}+A_2e^{-k_2t}) \tag{1}$$

where M is the drug dose (mg/m^2 or ug/g), M_g is the dose (mg/m^2 or ug/g) used to fit the experimental data and to obtain the plasma pharmacokinetic parameters for the liposome: A_1, A_2, k_1, and k_2 [2,23]. Here, the concentration of liposomal drug is assumed to scale linearly to the dose M. The first term in the

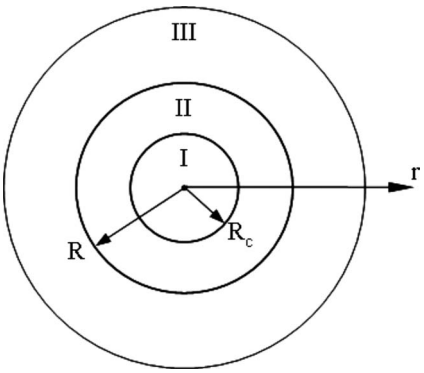

Fig. 3 Schematics of the tumor, I: central region of the tumor, II: peripheral region of the tumor, and III: surrounding normal tissue

Table 1 Parameters used in modeling

Parameters		Value
k_t		0.51 W/m K [27]
$(\rho c)_t$, $(\rho c)_b$		4180 J/m^3 K [28]
q_{met}		30,000 W/m^3 for tumor [28]
		450 W/m^3 for normal breast [29]
T_b		37°C
w_{b_37}		0 ml/s/ml in tumor central region
		0.009 ml/s/ml in tumor periphery [30]
		0.00018 ml/s/ml in normal tissue [30]
Mouse	M_g	6 μg/g [31]
	A_1	0
	A_2	90 μg/ml [31]
	k_1	0
	k_2	0.00033 min^{-1} [31]
Human	M_g	50 mg/m^2 [23]
	A_1	6.9 μg/ml [23]
	A_2	12.2 μg/ml [23]
	k_1	0.00502 min^{-1} [23]
	k_2	0.00025 min^{-1} [23]
$D_{L,\text{app}}$		2.4×10^{-9} cm^2/s [32]
P_{L_37}		2.0×10^{-8} cm/s [33]
S_t		200 cm^{-1} in tumor periphery [23]
		0 cm^{-1} in other regions
$D_{D,0}$		6.7×10^{-7} cm^2/s [34]
φ_{e0}		0.12 in central tumor [8]
		0.23 in tumor periphery [8]
		0.3 in normal tissue [35]
τ_r		24 h [23]
$v_{\max}$		2.8 μg/ml/min [23]
k_i		13.7 μg/ml [23]
k_e		0.219 μg/ml [23]
k_d		8.53×10^{-8} ml/μg/s [36]
C_1		743×10^8 [37]
α		0.000529 mm^{-1} [37]

brackets on the right hand side of the equation represents an initial rapid distribution phase of drug, where a minor fraction of the injected dose (A_1) is cleared through circulation with the kinetic parameter k_1. The second term is an extended distribution phase, where the rest of the dose (A_2) is cleared with the parameter k_2. Previous experimental research has found different values of pharmacokinetic parameters (k_1,k_2) in mouse and in human [26], which are listed in Table 1.

The liposomal drug in blood transports across the leaky wall of vessels and into the tumor interstitial through both diffusion and convection [38,39]. The apparent permeability $P_{L,\text{app}}$ of the vasculature is normally used to quantify the transvascular transport [40]. According to the definition, transvascular mass transfer of liposomal drug is proportional to the apparent vascular permeability, the concentration difference across the vessel wall, and the vessel surface area. A source term is used to describe the vascular leakage in the tumor peripheral region ($R_c<r<R$). In reference to the greatly enhanced extravasation of liposome previously found during hyperthermia [12], an increase of 76-fold in $P_{L,\text{app}}$ from its original value at 37°C is assumed. After the extravasation, liposomal drug transports in the interstitial space in both directions toward the central region and the surrounding normal tissue, respectively, owing to the concentration gradient (diffusion) and the motion of interstitial fluid (convection). For macromolecules like liposome, the magnitude of diffusion is comparable to the convection, and both should be considered. As it is hard to separate the diffusion and convection, an apparent diffusivity, $D_{L,\text{app}}$, is used to describe the interstitial transport process. In the mean time, the liposome ruptures and releases free antitumor drugs. This process is assumed to follow the first-order kinetics with the decaying time constant τ_r [23]. Thus, the concentration of the liposomal drug in the interstitial of the peripheral region can be determined by

$$\frac{\partial C_{L,E}}{\partial t} = D_{L,\text{app}} \cdot \nabla^2 C_{L,E} + P_{L,\text{app}} \cdot A_t (C_{L,V} - C_{L,E}) - C_{L,E}/\tau_r \quad (2)$$

where $C_{L,E}$ is the drug concentration in liposome form in the extracellular space (milligrams per milliliter of total tumor volume); the first term on the right hand side of the equation represents apparent diffusion of liposomal drug in tumor tissue, the second term the penetrative transport across the vessel wall, and the third term the rupture of liposome. A_t is the effective surface area of the vasculature per unit tumor volume.

Released from liposome, the antitumor drug (i.e., doxorubicin) transports in the interstitial space and is up-taken by the cells. For small molecules, such as doxorubicin, diffusion is dominant while convection is relatively smaller [41]. Moreover, high interstitial pressure in the tumor interior impedes convective transport of the drug. Therefore, convection is negligible for free doxorubicin transport. By considering tumor tissue as a porous material, the effective diffusivity of free drug D_D can be determined from the drug diffusivity in the interstitial fluid $D_{D,0}$ and the interstitial volume fraction φ_e [42]

$$D_D = \frac{2\varphi_e}{3-\varphi_e} D_{D,0} \quad (3)$$

As more and more tumor cells undergo necrosis or apoptosis during or post-treatment, the interstitial volume fraction φ_e increases [43] and is assumed to change linearly with tumor cell survival rate S

$$\varphi_e = 1 - (1 - \varphi_{e0}) \times S \quad (4)$$

where φ_{e0} is the initial volume fraction of interstitial space before drug treatment. Through the histological study, different values of φ_{e0} have been found in different regions of the tumor. S is the survival rate of the tumor cells.

Thus, the transport of free drug released from liposome can be expressed as

$$\frac{\partial C_{D,E}}{\partial t} = D_D \cdot \nabla^2 C_{D,E} + \frac{C_{L,E}}{\tau_r} - \frac{\partial C_{D,I}}{\partial t}(1-\varphi_e) \quad (5)$$

where $C_{D,E}$ is the free drug concentration in the extracellular space (milligrams per milliliter of total tumor volume); the first term on the right hand side represents free drug diffusion in tissue, the second term the drug released from liposome, and the third the cellular uptake of drug by the tumor cells, where $C_{D,I}$ is the intracellular bound drug concentration.

The drug is believed to transport passively across the cell membrane, and the cellular uptake is the carrier-mediated transport, which can be expressed as [23]

$$\frac{\partial C_{D,I}}{\partial t} = v_{\max}\left(\frac{C_{D,E}}{C_{D,E}+k_e} - \frac{C_{D,I}}{C_{D,I}+k_i}\right) \quad (6)$$

where $C_{D,I}$ is the intracellular bound drug concentration (milligrams per milliliter of intracellular volume). $v_{\max}$ is the maximal cellular uptake rate, and k_i and k_e are pharmacodynamics parameters.

Tumor is treated with both heating and drug. Since in vitro experimental studies have showed no significant tumor cell death under the hyperthermic condition at 42°C alone, cell killing is assumed mainly due to the drug effect, $S=S_d$. According to the drug killing mechanism, the cell survival rate decreases exponentially with the area under the drug concentration curve, the time integral of $C_{D,I}$ (AUC). Thus, S_d is expressed as [36]

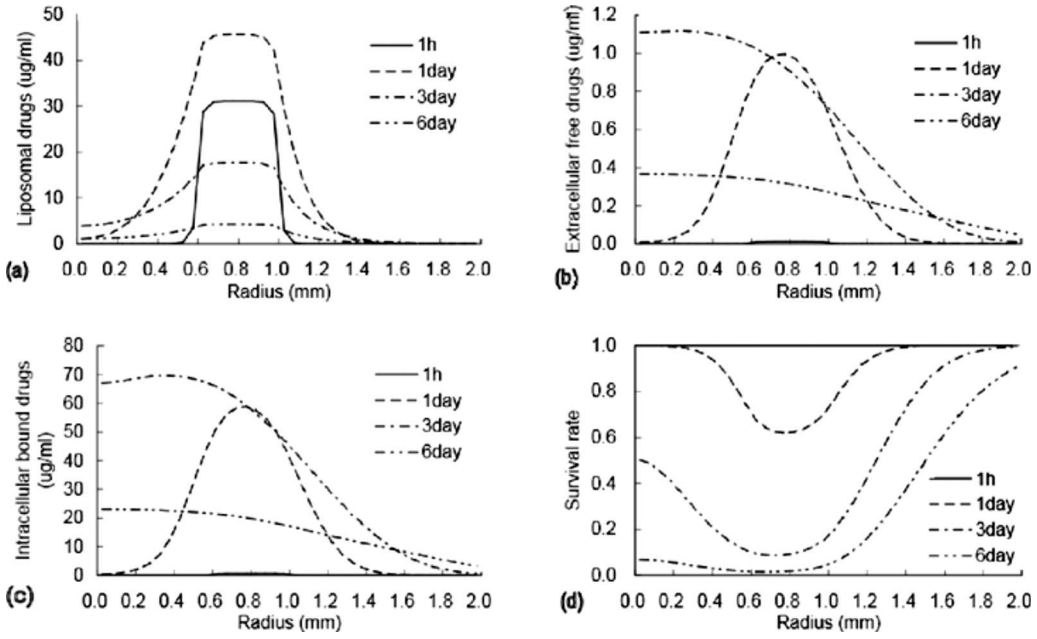

Fig. 4 Simulation results of drug concentration and cell survival rate in the tumor after 1 h liposomal drug delivery aided by hyperthermia at 42°C, where: the central region (0–0.6 mm), the peripheral region (0.6–1.0 mm), and the surrounding normal tissue (1.0–2.0 mm)

$$S_d = \exp\left(- k_d \times \int_0^t C_{D,I} dt \right) \tag{7}$$

where k_d is the pharmacodynamical parameter.

The corresponding boundary and initial conditions are listed as follows.

(1) For infinity,

$$C_{L,E}|_{r=\infty} = 0, \quad C_{D,E}|_{r=\infty} = 0, \quad C_{D,I}|_{r=\infty} = 0 \tag{8}$$

(2) For tumor center,

$$\left.\frac{\partial C_{L,E}}{\partial r}\right|_{r=0} = 0, \qquad \left.\frac{C_{D,E}}{\partial r}\right|_{r=0} = 0 \tag{9}$$

(3) For initial,

$$C_{L,E}|_{t=0} = 0, \quad C_{D,E}|_{t=0} = 0, \quad C_{D,I}|_{t=0} = 0 \tag{10}$$

4 Simulation Results and Discussion

The outcome of the animals treated by the thermally targeted nanoliposome drug delivery has been followed up and reported in Ref. [44]. The histological analysis finds no significant changes in the tumor cells in both the central and peripheral regions right after the heating. But 3 days later, many cells died in the peripheral region, while only a few dead cells were found in the central region. On the sixth day after drug administration, significant tumor cell death is found in both regions. The model developed above is first used to simulate the experimental results. According to the experiments, the tumor is about 1 mm in radius, and the radius of avascular central tumor is about 0.6 mm. With the parameters given in Table 1, Eqs. (1)–(7), the mass transfer of both liposomal and free drugs is numerically solved using MATLAB. Equations (1) and (2) are first solved to obtain $C_{L,E}$, and the results are substituted into Eq. (5). Equations (3)–(7) are solved simultaneously for $C_{D,E}$, $C_{D,i}$, and S. The spatial and temporal concentrations of both liposome and free drugs and the survival rate of the tumor cells are shown in Fig. 4.

As seen in Fig. 4(*a*), there is a great deal of liposomal drugs that accumulated in the peripheral region ($0.6 < r < 1.0$ mm) right after the heating. It decreases with time owing to its breakage and diffusion into the central region and the surrounding normal tissue. While in the central region ($0 < r < 0.6$ mm), the liposomal drug first increases, as the diffusion rate is faster than the rupture rate. But as more and more liposomes break and diffuse, and less come in from blood circulation, its concentration deceases again. The highest concentration in the central region appears 31.5 h after the treatment. The concentrations of free drug released from liposomes in both the peripheral and central regions first increase with time and then decrease (Fig. 4(*b*)). The highest concentration occurs after 42 h in the peripheral region and 70.5 h in the central region. The concentration of the intracellular bound drug changes synchronously with that of the extracellular free drug because of the relatively fast uptake process as compared with drug diffusion (Fig. 4(*c*)).

Numerical results shown in Fig. 4(*d*) indicate that right after the treatment, all the cells are alive. One day later, the drug effect on the tumor cells in the peripheral region appears, and the averaged survival rate decreases to 0.65 in this region. While very little doxorubicin has reached the central region, the average survival rate of the tumor cells is 0.94. On the third day, the survival rate of the tumor cells in the periphery gets even smaller with an average value of 0.10. An obvious decrease in the survival rate in the central tumor also occurs, and the average is 0.30. In 6 days, the survival rate in both regions further decreases, and the average becomes 0.01 and 0.04, respectively, indicating significant cell death. These predictions are in good agreement with the experimental findings reported in Ref. [44].

Furthermore, the model can also be used to predict the treatment effect of a relatively larger tumor (i.e., >1 cm in radius), in which it is more difficult for drug transport to the center. The model presented above has been used to predict drug distribution and the corresponding cell survival rate. With the administered dose (M) of 50 mg/m^2, the drug transport processes in a tumor 1 cm in radius without and with hyperthermia have been simulated, and the results are shown in Figs. 5 and 6, respectively.

As seen in Fig. 5, liposomal and free drugs mainly accumulate in the tumor periphery (6–10 mm). Little drug diffuses into the

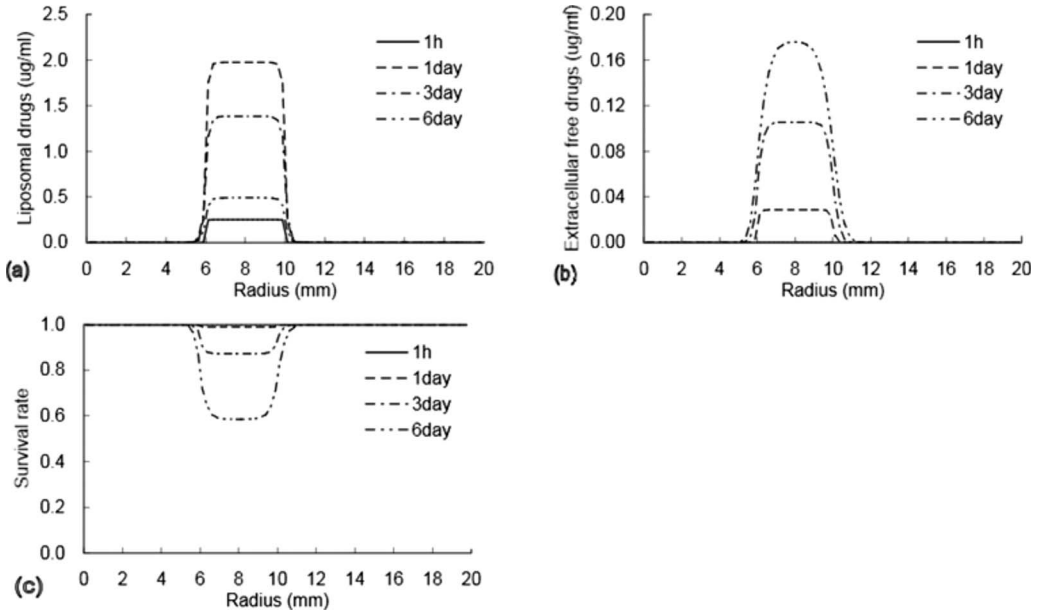

Fig. 5 Simulation results of drug concentrations and cell survival rate in a 1 cm tumor without hyperthermia, where: the central region (0–6 mm), the peripheral region (6–10 mm), and the surrounding normal tissue (10–20 mm)

center even in 6 days after the treatment, thus barely any cells die in the region. Even in the peripheral region, the cell death is insufficient due to the tumor size.

The transport process of liposomal drug after 1 h delivery with hyperthermia at 42°C is simulated, and the corresponding results are shown in Fig. 6. In comparison, the overall trend is quite similar except for the magnitude of the drug concentration and the cell survival rate. The locally imposed hyperthermia has greatly enhanced the accumulation of both the liposomal and free drugs in the peripheral region and resulted in a more serious damage in this region. In 6 days after the treatment, the averaged AUC of the liposomal drug under hyperthermia is about four times of that without hyperthermia, and the survival rate of the tumor cells in the peripheral region is almost 0. However, owing to the impermeability of the tumor mature vessels in the central region and the difficulty of liposomal drug diffusion, as predicted using the model, the drug effect in the tumor center is very limited even with local hyperthermia [31,35].

Encapsulating antitumor drug in liposomes delays the drug release and thus reduces the clearance rate of the drug in vivo. There have been a lot of efforts spent on improving the pharmacokinetics performance of liposomal drugs. Long circulation and ther-

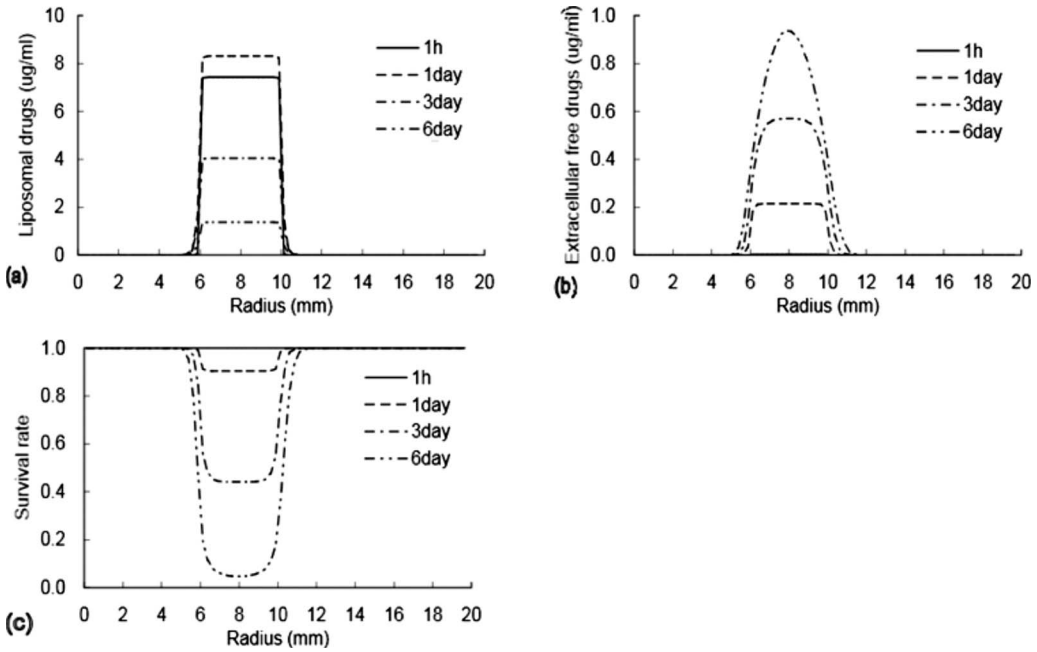

Fig. 6 Simulation results of drug concentrations and cell survival rate in a 1 cm tumor with hyperthermia, where: the central region (0–6 mm), the peripheral region (6–10 mm), and the surrounding normal tissue (10–20 mm)

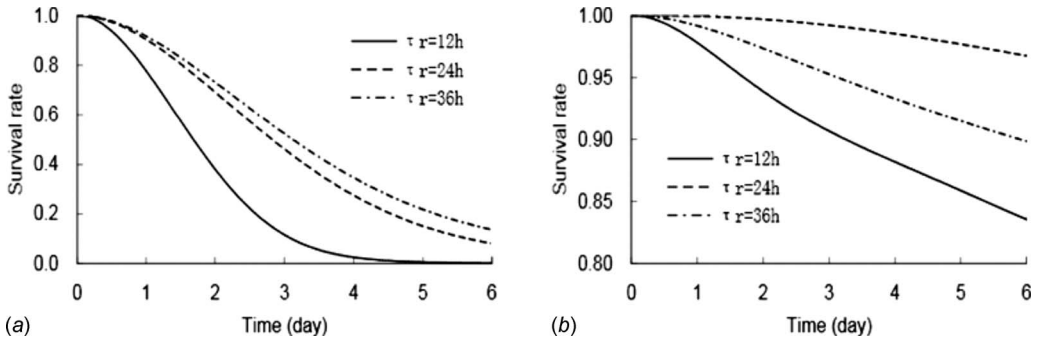

Fig. 7 The effect of liposome rupture time τ_r on drug delivery and tumor therapy: (*a*) average survival rate in the central region of the tumor and (*b*) average survival rate in the peripheral region of the tumor

mosensitive liposome have been developed. The speed of liposomal drug release also influences the treatment. To evaluate the liposome rupture influence, τ_r of 12 h and 36 h are used in the simulation. The numerical results of the average cell survival rate in the peripheral and central regions of tumor are shown in Fig. 7. It is noted that smaller value of τ_r results in better treatment efficacy in both regions. These predictions are in accordance with the experimental findings reported in Ref. [12] where temperature-sensitive liposomal drugs are proven to be more effective.

Different from other models [15,16,18], the present model accounts for the drug induced cell apoptosis or necrosis effect on the drug penetration using a cell survival rate dependent diffusion rate in Eqs. (3) and (4). Figure 8 illustrates the survival rate in the tumor center when the cell necrosis induced diffusivity change (CNIDC) is or is not taken into consideration. Significant difference can be found. As more cells die, the tissue porosity increases and thus the diffusivity. More drugs reach the rest of the tumor cells resulting in more cell death. The results indicate that the influence of the apoptosis or necrosis is an important parameter determining the accuracy of the prediction.

The above study has shown that the thermally targeted drug delivery enhanced the treatment effect of tumor. But, it is still difficult for the drug to diffuse to the central region in a relatively larger tumor and achieve the desired therapeutic effect. This finding is consistent with that reported from previous clinical studies [9,45]. For a complete ablation of large tumors, its central region needs to be treated by other modalities combined, i.e., high temperature or low temperature approaches [46].

5 Study of the Combined RF Ablation With Liposome Drug Treatment of Tumor

Previous clinical studies have shown that the combined RF ablation and liposomal doxorubicin treatment can be used to enhance the delivery of liposomal drugs and to maximize the tumor destruction [46]. To optimize the combined treatment, both the temperature and drug induced cell necrosis need to be considered, thus the coupled temperature and drug distributions after the treatment are of a great importance. The present model is used to simulate the combined RF ablation and liposomal doxorubicin delivery for a tumor 1 cm in diameter. The RF probe, guided by the imaging system, is inserted into the center of the tumor right after intravenous delivery of the liposomal drugs. During the RF treatment, the temperature distribution inside the tumor is analyzed using the Pennes bioheat transfer equation, in which the RF volumetric heating is treated as the source [47]

$$(\rho c)_t \frac{\partial T_t}{\partial t} = k_t \nabla^2 T_t + \omega_b (\rho c)_b (T_b - T_t) + q_{\mathrm{SAR}} + q_{\mathrm{met}} \qquad (11)$$

where T_t is the tissue temperature. k_t is the thermal conductivity, ρ is the density, c thermal capacity, subscript t refers to tissue and b to blood, w_b is the blood perfusion rate, T_b is the blood temperature, and q_{SAR} and q_{met} are the specific absorption rates of the RF heating and the metabolic heat, respectively. k_t, ρ, and c are assumed to be the same in all the regions, while different w_b and q_{met} values are used, as shown in Table 1. Sensitivity of the blood perfusion rate to temperature is considered. From previous experiments, it has been found that blood flow increases to about twofold of w_{b_37} (w_b at 37°C) at 42°C [30] and fourfold of w_{b_37} at 44°C [30]. It stops at temperatures either lower than 8°C [48] or higher than 46°C [30]. The blood perfusion w_b is assumed to change linearly between these temperature points. By considering the RF probe as a finite line source, the specific absorption rate of RF in tissue, q_{SAR}, can be expressed as [37]

$$q_{\mathrm{SAR}} = C_1 p \frac{(2\alpha r + n - 2)e^{-2\alpha r}}{r^n} e^{-z^2/z_c^2} \qquad (12a)$$

where z and z_c are the axial distance and the decay distance, respectively, p is the RF power, C_1 is the scaling constant, α is the attenuation constant, n is an exponential constant, and r is the radial distance from the center. Referring to the experimental measurements reported in Ref. [49], the specific adsorption rate of the RF heating is simplified as

$$q_{\mathrm{SAR}} = \begin{cases} C_1 p \dfrac{(0.001058r + 1)e^{-0.001058r}}{r^3} & -z_0 \le x \le z_0 \\ 0 & \text{else} \end{cases} \qquad (12b)$$

where z_0 is the active length of the RF probe; it varies with tumor dimensions. The probe diameter is 3 mm. Values of the parameters used are shown in Table 1. To overcome local overheating, the RF probes with internal cooling are normally used [49,50]. In this study, the convective condition between the probe wall and

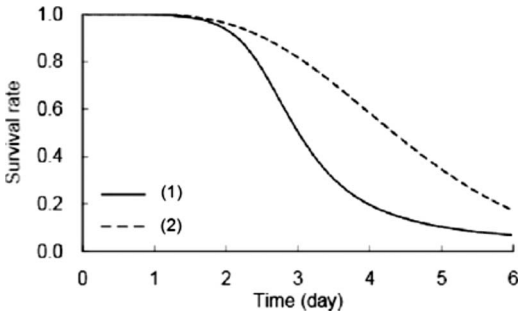

Fig. 8 The effect of cell necrosis induced diffusivity change on tumor therapy: (1) with cell necrosis induced diffusivity change considered; (2) without consideration of cell necrosis induced diffusivity change

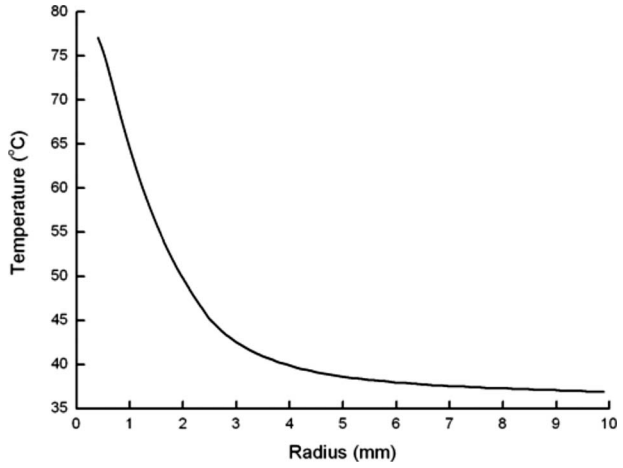

Fig. 9 Temperature distribution in the tumor after 30 min of the RF heating at 10 W; radius represents the distance measured from the RF probe

the flow inside the probe is adopted from Ref. [49], in which low temperature nitrogen is used. The boundary condition for tissue contacting the probe surface is

$$k_t \frac{\partial T_t}{\partial r} = h_g(T_t - T_i) \quad \text{at} \quad r = r_0, z > -z_0 \tag{13}$$

where T_i is the inner-flow temperature, h_g is the internal convection coefficient of the flow, and r_0 is the probe radius.

The apparent vascular permeability, $P_{L,\text{app}}$, is assumed to change linearly with temperature from the initial value P_{L_37} at 37°C to 76-fold P_{L_37} at 42°C [12], and kept until 44°C, when the blood flow starts to drop [51] and decreases linearly to zero at 46°C. During the heating period, the tumor cells are killed through heating, as the drugs are mainly enclosed in liposomes and have not taken into effect. Heating induced survival rate of the tumor cells S_h is

$$S_h = e^{-k_h \int_0^t R^{(43-T)} d\tau} \tag{14}$$

where k_h and R are constants. After heating, the tumor cells that survived are subsequently killed by antitumor drugs. Thus, the total survival rate of cells, S, is expressed as

$$S = S_h \times S_d \tag{15}$$

The partial differential equations (PDEs) governing the unknowns are essentially nonlinear, especially for the RF ablation combined drug delivery process when the apparent permeability, $P_{L,\text{app}}$, and S are also temperature dependent. The distribution of temperature and drug concentration in the tumor and surrounding normal tissue in different time intervals are then numerically obtained using FLUENT.

Temperatures at different distances from the RF probe in the tumor after 30 min of heating are shown in Fig. 9. It can be seen that tissue temperatures in the central region ($0.25 \text{ mm} < r < 2.5 \text{ mm}$) are all above 45°C, and can reach as high as 78°C near the probe in the center, while in the peripheral region ($2.5 \text{ mm} < r < 5 \text{ mm}$) tissue temperatures are between 37°C and 45°C. It is hard to further increase the tissue temperature due to a rapid decay in the RF heating and the much higher local blood perfusion in the periphery.

Distributions of liposomal drug, extracellular free drug, and the survival rate of the tumor cells in different days after the combined RF ablation and liposome drug treatment are shown in Figs. 10(*a*)–10(*c*). Obviously, the liposomal drug mainly concentrates in the peripheral region. Much less liposomal drug extravasates in the central region or in the surrounding normal tissue because of the absence of blood vessels in the tumor center and the low permeability of the vessel wall in normal tissue. The concentration of liposomal drug in the periphery decreases with time due to the decay of liposome concentration in blood and the rupture of liposomes. In 7 days after the treatment, the interstitial liposomal drug concentration decreases to 1.0 μg/ml, and most liposomes rupture. As seen in Fig. 10(*b*), the concentration of the extracellular free drug first increases in the peripheral region, and then decreases as diffusion into the central region. While in the central region, as most of the cells have been killed by the RF heating, only drug diffusion takes place and also decreases later when the source decreases. The cell survival rates with respect to time are shown in Fig. 10(*c*). Most of the tumor cells have been killed right after the RF ablation, while those in the peripheral region are gradually killed by the liposomal drug. The simulation results show that the combined RF ablation and liposomal drug treatment of the tumor could achieve much better treatment effect by overcoming the disadvantages of either one alone, especially for a sizable tumor. The major concern of the RF ablation alone is the increased blood perfusion in the tumor peripheral region during heating, which might result in incomplete killing and increase certain risks of the incidence of tumor metastasis [52,53]. The thermally enhanced extravasation of the nanoliposome drugs could ensure sufficient killing of the surviving tumor cells and vasculature in the peripheral region.

For larger tumors, the heating power of the RF can be increased, and local overheating be prevented by adjusting the flow rate of low temperature nitrogen inside the RF probe. Figure 11 illustrates the extravasation of the liposome drug right after the RF heating of a 3 cm diameter tumor and the survival rate of the tumor cells in 7 days after the combined treatment with different heating powers. Obviously, for the heating powers studied, the higher the power, the more liposome drugs extravasated in the peripheral region, and the more tumor cells that die. In the outer central region of tumor, there is a peak on the curve of the tumor cell survival rate shown in Fig. 11(*b*) for powers that are relatively low. In this region, the temperature increase is not high enough, and the drug fails to have a fatal effect. When the power is increased to 60 W, the highest temperature inside the tumor reaches about 87°C; most of the tumor cells in the central region could be completely killed, but not in the peripheral region, where the cells are mainly killed by the drug. By decreasing the half-life time of the liposome drug τ_r, the survival rate of the tumor cells in this region is significantly decreased, indicating a great potential of the thermally sensitive liposome drug.

The total volume of the tumor cells (3 cm diameter), with the survival rate lower than 0.1%, after the RF ablation alone is compared with that of the combined treatment, as shown in Fig. 12. The treatment region is clearly enlarged through the latter, which accords well with the experimental findings reported in Ref. [46]. On the other hand, it is worthy noting that for the combined treatment, besides the RF heating power and the half-life time of the liposome drug, as studied in this paper, the timing of the liposome drug delivery in relation to the RF ablation is another important factor that would affect the final therapeutic outcome [46].

6 Conclusion

A new mathematical model has been developed to study the thermally targeted drug delivery process in tumor. Both the drug distribution and the treatment efficacy under different treatment protocols have been numerically simulated. The influence of several key parameters on drug delivery and therapeutic efficiency are discussed.

Local hyperthermia enhances the accumulation of liposomal drugs in the tumor region by increasing tumor vessel permeability $P_{L,\text{app}}$ and blood perfusion. Numerical results show higher AUC of liposomal drugs in tumor tissue under the hyperthermic condition. Compared with liposomes, the diffusion of free drug contributes more to drug transport in tumor tissue, since the diffusivity of

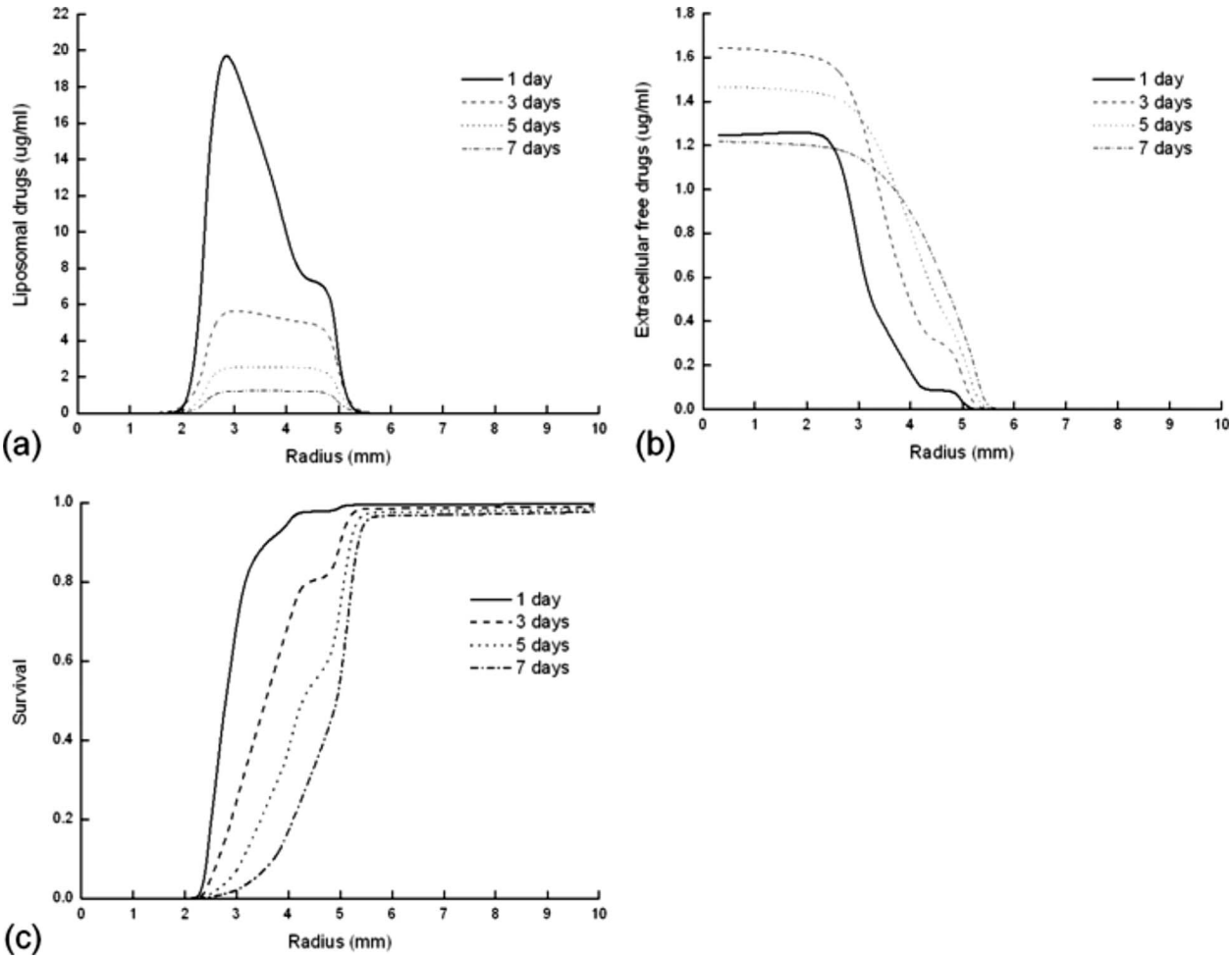

Fig. 10 Simulation results of drug concentrations and cell survival rate distribution in a 1 cm tumor under the combined RF ablation with the liposome drug treatment, where: the central region (0–2.5 mm), the peripheral region (2.5–5 mm), and the normal tissue (5–10 mm). Heating power is 10 W.

free drugs, D_D, is much bigger than the apparent diffusivity of liposome, $D_{L,\mathrm{app}}$. Furthermore, the drug induced cell apoptosis or necrosis improves the diffusivity of free drug so as to improve drug transport in tissue. Such an effect is significant and should be considered for an accurate prediction of the therapeutic effect.

For tumors larger than 1 cm, hyperthermia can only help accu-

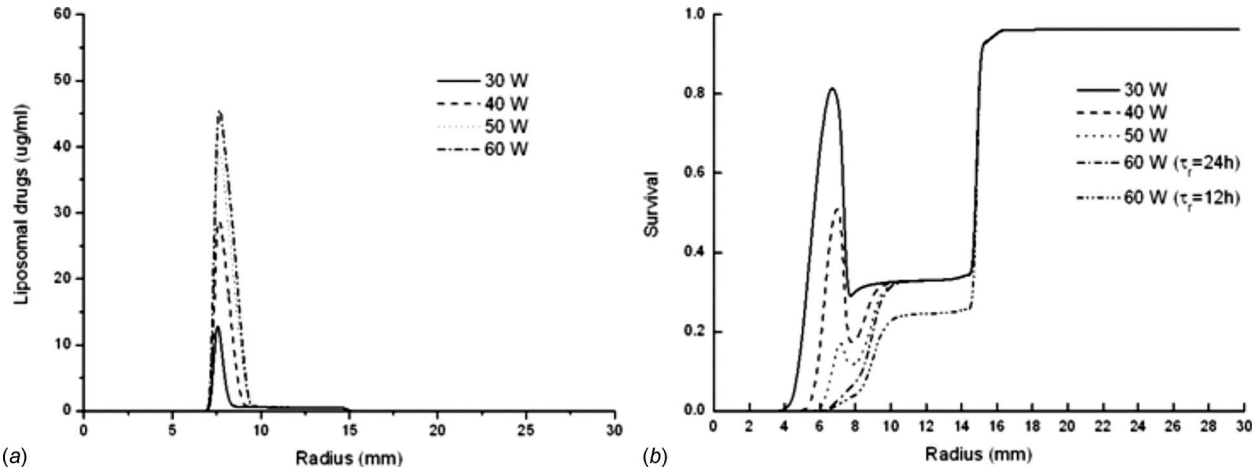

Fig. 11 Simulation results of drug concentrations and cell survival rates in a 3 cm diameter tumor under various powers of the RF heating. (*a*) Concentration of the liposome drug in tumor right after the RF heating, (*b*) tumor cell survival rates in 7 days after the combined treatments for different powers of the RF heating and different half-life times of liposome drug, where: the central region (0–7.5 mm), the peripheral region (7.5–15 mm), and the normal tissue (15–30 mm).

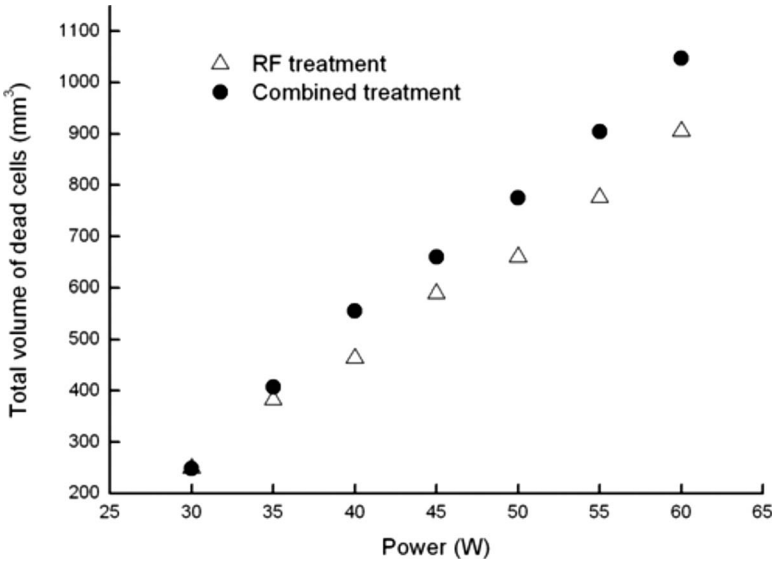

Fig. 12 The total volume of the tumor cells with the survival rate lower than 0.1% after the RF ablation alone and the combined treatment using different heating powers

mulate more antitumor drug in the peripheral region. Insufficient drug in the central region can be overcome through combined RF ablation in the tumor center. But, to reach the complete destruction of the tumor, a detailed treatment planning is needed, especially for tumors with irregular shapes. The present model can be further used to simulate the transport of other nanoparticles or quantum dots in tissue.

Acknowledgment

This work has been supported by the National Natural Science Foundation of China (Contract Nos. 50506016 and 50725622) and Ministry of Science and Technology of China (Contract Nos. 2006CB0D0100 and 2009CB930400).

Nomenclature

C = concentration of the drug
M = drug dose
t = time
D = diffusion coefficient
$P_{L,\mathrm{app}}$ = apparent permeability of the vasculature
A = surface area
S = survival rate
T = temperature
k = thermal conductivity
c = thermal capacity
q_{SAR} = specific absorption rate of the RF heating
q_{met} = metabolic heat
h = convection coefficient
z = axial distance
z_c = axial decay distance
p = RF power

Greek Symbols

ρ = density
φ = volume fraction of interstitial space
ω = blood perfusion rate
$v_{\max}$ = the maximum cellular uptake rate

Subscripts

L = liposome
D = free antitumor drug
E = extracellular
I = intracellular
t = tissue
b = blood
h = heat
d = drug

References

[1] Szoka, F. C., 1991, "Liposomal Drug Delivery: Current Status and Future Prospects," *Membrane Fusion*, J. Wilschut and D. Hoekstra, eds., Marcel Dekker, New York, pp. 845–890.
[2] Gabizon, A., Catane, R., Uziely, B., Kaufman, B., Safra, T., Cohen, R., Martin, F., Huang, A., and Barenholz, Y., 1994, "Prolonged Circulation Time and Enhanced Accumulation in Malignant Exudates of Doxorubicin Encapsulated in Polyethylene-Glycol Coated Liposomes," Cancer Res., **54**(4), pp. 987–992.
[3] Nagayasu, A., Uchiyama, K., and Kiwada, H., 1999, "The Size of Liposomes: A Factor Which Affects Their Targeting Efficiency to Tumors and Therapeutic Activity of Liposomal Antitumor Drugs," Adv. Drug Delivery Rev., **40**(1–2), pp. 75–87.
[4] Kong, G., Braun, R. D., and Dewhirst, M. W., 2000, "Hyperthermia Enables Tumor-Specific Nanoparticle Delivery: Effect of Particle Size," Cancer Res., **60**(16), pp. 4440–4445.
[5] Ning, S., Macleod, K., Abra, R. M., Huang, A. H., and Hahn, G. M., 1994, "Hyperthermia Induces Doxorubicin Release From Long-Circulating Liposomes and Enhances Their Anti-Tumor Efficacy," Int. J. Radiat. Oncol., Biol., Phys., **29**(4), pp. 827–834.
[6] Dvorak, J., Zoul, Z., Melichar, B., Petera, J., Vesely, P., Vosmik, M., and Dolezel, M., 2004, "Liposomal Doxorubicin Combined With Regional Hyperthermia: Reducing Systemic Toxicity and Improving Locoregional Efficacy in the Treatment of Solid Tumors," J. Chemother., **16**, pp. 34–36.
[7] Urano, M., Kuroda, M., and Nishimura, Y., 1999, "For the Clinical Application of Thermochemotherapy Given at Mild Temperatures," Int. J. Hyperthermia, **15**(2), pp. 79–107.
[8] Liu, P., Zhang, A., Xu, Y., and Xu, L. X., 2005, "Study of Non-Uniform Nanoparticle Liposome Extravasation in Tumor," Int. J. Hyperthermia, **21**(3), pp. 259–270.
[9] Kong, G., and Dewhirst, M. W., 1999, "Hyperthermia and Liposomes," Int. J. Hyperthermia, **15**(5), pp. 345–370.
[10] Xu, L. X., Zhu, L., and Holmes, K. R., 1998, "Thermoregulation in the Canine Prostate During Transurethral Microwave Hyperthermia, Part I: Temperature Response," Int. J. Hyperthermia, **14**(1), pp. 29–37.
[11] Maruyama, K., Unezaki, S., Takahashi, N., and Iwatsuru, M., 1993, "Enhanced Delivery of Doxorubicin to Tumor by Long-Circulating Thermosensitive Liposomes and Local Hyperthermia," Biochim. Biophys. Acta, **1149**(2), pp. 209–216.
[12] Gaber, M. H., Wu, N. Z., Hong, K., Huang, S. K., Dewhirst, M. W., and Papahadjopoulos, D., 1996, "Thermosensitive Liposomes: Extravasation and Release of Contents in Tumor Microvascular Networks," Int. J. Radiat. Oncol., Biol., Phys., **36**(5), pp. 1177–1187.
[13] Ribba, B., Marron, K., Agur, Z., Alarcon, T., and Maini, P. K., 2005, "A Mathematical Model of Doxorubicin Treatment Efficacy for Non-Hodgkin's Lymphoma: Investigation of the Current Protocol Through Theoretical Mod-

elling Results," Bull. Math. Biol., **67**(1), pp. 79–99.
[14] Tzafriri, A. R., Lerner, E. I., Flashner-Barak, M., Hinchcliffe, M., Ratner, E., and Parnas, H., 2005, "Mathematical Modeling and Optimization of Drug Delivery From Intratumorally Injected Microspheres," Clin. Cancer Res., **11**, pp. 826–834.
[15] Ward, J. P., and King, J. R., 2003, "Mathematical Modelling of Drug Transport in Tumor Multicell Spheroids and Monolayer Cultures," Math. Biosci., **181**(2), pp. 177–207.
[16] Lankelma, J., Luque, R. F., Dekker, H., Schinkel, W., and Pinedo, H. M., 2000, "A Mathematical Model of Drug Transport in Human Breast Cancer," Microvasc. Res., **59**(1), pp. 149–161.
[17] Lankelma, J., Luque, R. F., Dekker, H., and Pinedo, H. M., 2003, "Simulation Model of Doxorubicin Activity in Islets of Human Breast Cancer Cells," Biochim. Biophys. Acta, **1622**(3), pp. 169–178.
[18] Magni, P., Simeoni, M., Poggesi, I., Rocchetti, M., and De Nicolao, G., 2006, "A Mathematical Model to Study the Effects of Drugs Administration on Tumor Growth Dynamics," Math. Biosci., **200**(2), pp. 127–151.
[19] El-Kareh, A. W., and Secomb, T. W., 2003, "A Mathematical Model for Cisplatin Cellular Pharmacodynamics," Neoplasia, **5**(2), pp. 161–169.
[20] El-Kareh, A. W., and Secomb, T. W., 2005, "Two-Mechanism Peak Concentration Model for Cellular Pharmacodynamics of Doxorubicin," Neoplasia, **7**(7), pp. 705–713.
[21] El-Kareh, A. W., and Secomb, T. W., 2004, "A Theoretical Model for Intraperitoneal Delivery of Cisplatin and the Effect of Hyperthermia on Drug Penetration Distance," Neoplasia, **6**(2), pp. 117–127.
[22] Maruyama, K., Ishida, O., Takizawa, T., and Moribe, K., 1999, "Possibility of Active Targeting to Tumor Tissues With Liposomes," Adv. Drug Delivery Rev., **40**(1–2), pp. 89–102.
[23] El-Kareh, A. W., and Secomb, T. W., 2000, "A Mathematical Model for Comparison of Bolus Injection, Continuous Infusion, and Liposomal Delivery of Doxorubicin to Tumor Cells," Neoplasia, **2**(4), pp. 325–338.
[24] Lankelma, J., Dekker, H., Luque, F. R., Luykx, S., Hoekman, K., van der Valk, P., van Diest, P. J., and Pinedo, H. M., 1999, "Doxorubicin Gradients in Human Breast Cancer," Clin. Cancer Res., **5**(7), pp. 1703–1707.
[25] Jang, S. H., Wientjes, M. G., Lu, D., and Au, J. L., 2003, "Drug Delivery and Transport to Solid Tumors," Pharm. Res., **20**(9), pp. 1337–1350.
[26] Gabizon, A., Shmeeda, H., and Barenholz, Y., 2003, "Pharmacokinetics of Pegylated Liposomal Doxorubicin—Review of Animal and Human Studies," Clin. Pharmacokinet, **42**(5), pp. 419–436.
[27] Elliott, G. D., and McGrath, J. J., 1999, "Freezing Response of Mammary Tissue: A Mathematical Study," Heat Mass Transfer, **44**, pp. 59–64.
[28] Chato, J. C., 1987, "Thermal Properties of Tissues," *Handbook of Bioengineering*, Vols. 9.1–9.13, R. Skalak and S. Chien, eds., McGraw-Hill, New York.
[29] Zhang, A., Xu, L. X., Sandison, G. A., and Zhang, J., 2003, "A Microscale Model for Prediction of Breast Cancer Cell Damage During Cryosurgery," Cryobiology, **47**(2), pp. 143–154.
[30] Xu, L. X., Zhu, L., and Holmes, K. R., 1998, "Thermoregulation in the Canine Prostate During Transurethral Microwave Hyperthermia, Part II: Blood Flow Response," Int. J. Hyperthermia, **14**(1), pp. 65–73.
[31] Siegal, T., Horowitz, A., and Gabizon, A., 1995, "Doxorubicin Encapsulated in Sterically Stabilized Liposomes for the Treatment of a Brain Tumor Model: Biodistribution and Therapeutic Efficacy," J. Neurosurg., **83**(6), pp. 1029–1037.
[32] Nugent, L. J., and Jain, R. K., 1984, "Extravascular Diffusion in Normal and Neoplastic Tissues," Cancer Res., **44**(1), pp. 238–244.
[33] Yuan, F., Leunig, M., Huang, S. K., Berk, D. A., Papahadjopoulos, D., and Jain, R. K., 1994, "Microvascular Permeability and Interstitial Penetration of Sterically Stabilized (Stealth) Liposomes in a Human Tumor Xenograft," Cancer Res., **54**(13), pp. 3352–3356.
[34] Qian, F., Stowe, N., Liu, E. H., Saidel, G. M., and Gao, J., 2003, "Quantification of In Vivo Doxorubicin Transport From PLGA Millirods in Thermoablated Rat Livers," J. Controlled Release, **91**(1–2), pp. 157–166.
[35] El-Kareh, A. W., and Secomb, T. W., 2004, "A Theoretical Model for Intraperitoneal Delivery of Cisplatin and the Effect of Hyperthermia on Drug Penetration Distance," Neoplasia, **6**(2), pp. 117–127.
[36] Tsuchihashi, M., Harashima, H., and Kiwada, H., 1999, "Development of a Pharmacokinetic/Pharmacodynamic (PK/PD)-Simulation System for Doxorubicin in Long Circulating Liposomes in Mice Using Peritoneal P388," J. Controlled Release, **61**(1–2), pp. 9–19.
[37] Zhu, L., Mi, Z., and Xu, L. X., 1998, "Temperature Distribution in Prostate During Transurethral Radio Frequency Thermotherapy Treatment of Benign Prostatic Hyperplasia," *Advances in Heat Mass Transfer in Biotechnology*, HTD-Vol.362/BED-Vol.40, ASME, New York, NY, pp. 117–122.
[38] Jain, R. K., 1987, "Transport of Molecules Across Tumor Vasculature," Cancer Metastasis Rev., **6**(4), pp. 559–593.
[39] Chen, B., and Fu, B. M., 2004, "An Electrodiffusion-Filtration Model for Effects of Endothelial Surface Glycocalyx on Microvessel Permeability to Macromolecules," ASME J. Biomech. Eng., **126**(5), pp. 614–624.
[40] Dreher, M. R., Liu, W., Michelich, C. R., Dewhirst, M. W., Yuan, F., and Chilkoti, A., 2006, "Tumor Vascular Permeability, Accumulation, and Penetration of Macromolecular Drug Carriers," J. Natl. Cancer Inst., **98**(5), pp. 335–344.
[41] El-Kareh, A. W., and Secomb, T. W., 1997, "Theoretical Models for Drug Delivery to Solid Tumors," Crit. Rev. Biomed. Eng., **25**(6), pp. 503–571.
[42] El-Kareh, A. W., Braunstein, S. L., and Secomb, T. W., 1993, "Effect of Cell Arrangement and Interstitial Volume Fraction on the Diffusivity of Monoclonal Antibodies in Tissue," Biophys. J., **64**(5), pp. 1638–1646.
[43] Jang, S. H., Wientjes, M. G., Lu, D., and Au, J. L. S., 2003, "Drug Delivery and Transport to Solid Tumors," Pharm. Res., **20**(9), pp. 1337–1350.
[44] Liu, P., and Xu, L. X., 2006, "Enhanced Efficacy of Anti-Tumor Liposomal Doxorubicin by Hyperthermia," 28th Annual International Conference IEEE Engineering Medicine and Biology Society.
[45] Weinstein, J. N., Magin, R. L., Yatvin, M. B., and Zaharko, D. S., 1979, "Liposomes and Local Hyperthermia: Selective Delivery of Methotrexate to Heated Tumors," Science, **204**, pp. 188–191.
[46] Ahmed, M., and Goldberg, S. N., 2004, "Combination Radiofrequency Thermal Ablation and Adjuvant IV Liposomal Doxorubicin Increases Tissue Coagulation and Intratumoral Drug Accumulation," Int. J. Hyperthermia, **20**(7), pp. 781–802.
[47] Zhu, L., and Xu, L. X., 1999, "Evaluation of the Effectiveness of Transurethral RF Hyperthermia in the Canine Prostate: Temperature Distribution Analysis," ASME J. Biomech. Eng., **121**(6), pp. 584–590.
[48] Schuder, G., Pistorius, G., Fehringer, M., Feifel, G., Menger, M. D., and Vollmar, B., 2000, "Complete Shutdown of Microvascular Perfusion Upon Hepatic Cryothermia Is Critically Dependent on Local Tissue Temperature," Br. J. Cancer, **82**(4), pp. 794–799.
[49] Sun, J. Q., Zhang, A., and Xu, L. X., 2008, "Evaluation of Alternative Cooling and Heating for Tumor Treatment," Int. J. Heat Mass Transfer, **51**(23–24), pp. 5478–5485.
[50] Lee, J. M., Han, J. K., Kim, S. H., Lee, J. Y., Choi, S. H., and Choi, B. I., 2004, "Hepatic Bipolar Radiofrequency Ablation Using Perfused-Cooled Electrodes: A Comparative Study in the Ex Vivo Bovine Liver," Br. J. Radiol., **77**, pp. 944–949.
[51] Eddy, H. A., 1980, "Alterations in Tumor Microvasculature During Hyperthermia," Radiology, **137**(2), pp. 515–21.
[52] Greenstein, A., and Koontz, W. W., Jr., 2002, "Does Local Hyperthermia Affect Metastasis of a Human Prostate Carcinoma Grown in Athymic Nude Mice?," Int. J. Hyperthermia, **18**, pp. 285–291.
[53] Salsbury, A. J., 1975, "The Significance of the Circulating Cancer Cell," Cancer Treat Rev., **2**, pp. 55–72.